

# Photocatalytic Degradation of Azo Dye Acid Red 14 from Aqueous Solutions Using MWCNTs Nanocatalyst

Reza Moradi<sup>a\*</sup>, Kazem Mahanpoor<sup>b</sup>

<sup>a</sup>Young Researchers and Elite Club, Arak Branch, Islamic Azad University, Arak, Iran.

<sup>b</sup>Department of Chemistry, Arak Branch, Islamic Azad University, Arak, Iran.

\*Correspondence should be addressed to Dr. Reza Moradi, Email: [reza.moradi\\_bi@yahoo.com](mailto:reza.moradi_bi@yahoo.com)

## A-R-T-I-C-L-E-I-N-F-O

### Article Notes:

Received: Nov 28, 2017

Received in revised form:  
Apr 18, 2018

Accepted: Apr 28, 2018

Available Online: May 1,  
2018

### Keywords:

Dye,  
Acid Red 14,  
Experimental design,  
Photocatalytic Degradation,  
Carbon nanotubes,  
Iran.

## A-B-S-T-R-A-C-T

**Background & Aims of the Study:** Azo Dyes are the most hazardous materials in different industries. Dyes and pigments used in industries for applications such as textiles, leathers, papers, foodstuffs, additives, etc. Application amounts of azo dyes in industries which can cause severe health problems in human and environmental pollutant problems. So, color wastewaters decomposition plan are necessary. The purpose of this study is the application statistical experimental design in photocatalytic decomposition of azo dye Acid Red 14 (AR14) from aqueous solutions using multi walled carbon nanotubes (MWCNTs) particles which was used UV/H<sub>2</sub>O<sub>2</sub> process in photoreactor.

**Materials & Methods:** MWCNTs particles as a catalyst used for the degradation of dye in aqueous solution. MWCNTs particles have been characterized by scanning electron microscopy (SEM), Transmission Electron Microscopy (TEM) and Fourier transform infrared (FT-IR). Design of experimental (DOE) based design matrix was exerted for measure the effect of these three factors such as: A) pH, B) catalyst amount and C) H<sub>2</sub>O<sub>2</sub> concentration at two levels. The full factorial experimental design was utilized in this process. The significant effects of each factor and interactions determined using analysis of variance (ANOVA) method. The decomposition kinetic of dye was studied.

**Results:** The maximum photocatalytic degradation efficiency of dye obtained in this study was found 90.65%, corresponding to the optimal conditions of 3, 30 mg L<sup>-1</sup> and 20 ppm respectively, for the pH, catalyst amount and H<sub>2</sub>O<sub>2</sub> concentration. The most effective factor in the photocatalytic degradation efficiency was H<sub>2</sub>O<sub>2</sub> concentration. The interaction between pH×H<sub>2</sub>O<sub>2</sub> concentrations was the most effective interaction. A pseudo first order reaction with a rate constant ( $k=0.0696 \text{ min}^{-1}$ ) was observed for the photocatalytic degradation of dye.

**Conclusions:** The results showed that photodegradation process can be suitable alternative to degradation dyes in aqueous solutions.

**Please cite this article as:** Moradi R, Mahanpoor K. Photocatalytic Degradation of Azo Dye Acid Red 14 from Aqueous Solutions Using MWCNTs Nanocatalyst. Arch Hyg Sci 2018;7(2):71-80.

## Background

The color is a reflection of the interaction between visible light and matter. There are three criteria for color assessment such as: shades, brightness and depth (1). Azo dye Acid Red 14 is type's of acidic dyes. This group of dyes are solutions in water, and when dissolve in water, they are negatively charged, and salts

are organic acids (2). Dyes and pigments used in industries for applications such as textiles, leathers, papers, foodstuffs, additives, etc (3, 4). Azo dyes are toxic and dangerous because they have aromatic ring in their structure. The advanced oxidation processes (AOPs) methods for degradation of dyes in aqueous solution were studied by many investigators (5-8). The mixed use of CNTs and H<sub>2</sub>O<sub>2</sub> to a certain extent

yielded a significant improvement of dye photooxidation compared to that of the H<sub>2</sub>O<sub>2</sub> oxidation alone. H<sub>2</sub>O<sub>2</sub> can be activated on the CNTs surface to generate hydroxyl free radicals. The CNTs is an electron-transfer catalyst. The catalytic decomposition of H<sub>2</sub>O<sub>2</sub> by CNTs involves the exchange of a surface hydroxyl group on CNTs surface with a hydrogen peroxide anion (HO<sub>2</sub><sup>-</sup>) to on the surface, which then decomposes another generate peroxide H<sub>2</sub>O<sub>2</sub> molecule producing oxygen and regenerating the CNTs active site (9-11). Recently, CNTs have attracted great interest as a new type of catalyst for removing environmental pollutants (12,13). The statistical methods are invaluable not only in the analysis of experimental data, but also in designing and optimizing experiments. The experimental design is usually used to describe the stages of (14):

1. Identifying the factors which may affect the result of an experiment.
2. Designing the experiment so that the effects of uncontrolled factors are minimized.
3. Using statistical analysis to separate and evaluate the effects of the different factors involved.

**Aims of the study:**

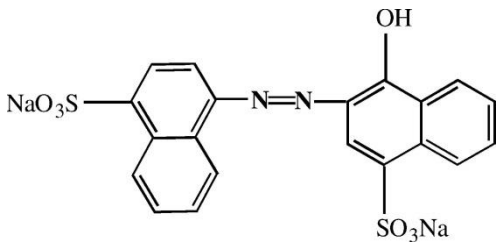
In this study, MWCNTs particles were characterized by SEM, TEM and FT-IR. The reaction kinetic was studied. The effects of operational factor such as pH, catalyst amount and H<sub>2</sub>O<sub>2</sub> concentration were studied using a 2<sup>3</sup> full factorial design with two levels (low and high) and three factors in order to examine the main effects and the interactions between operational factors in the photocatalytic degradation of AR14.

**Materials & Methods**

**Materials**

The mono azo dye, AR14 was obtained from Alvan Sabet Company (Iran) and was used without further purification. The structure and characteristics of AR14 is shown in Table 1. The pH values were adjusted at desired level using dilute NaOH and H<sub>2</sub>SO<sub>4</sub>. MWCNTs (appearance: black powder, length: 5–15 μm, outer diameter: 15–40 nm, purity (carbon): ≥92%, density: 0.03-0.16 g cm<sup>-3</sup>, and specific surface area (BET, N<sub>2</sub>): 127 m<sup>2</sup> g<sup>-1</sup>) was received from Research Institute of Petroleum Industry (Iran). Other chemicals used in the paper were purchased from the Merck Company (Germany). Double distilled water was used for preparation of requisite solutions.

**Table 1) The structure and characteristics of dye.**

Dye	Structure	C.I.	λ <sub>max</sub> (nm)	MW (g mol <sup>-1</sup> )
AR14		14720	514	502.423

15W (UV-C) was used. UV/Vis Spectrophotometer, Jenway (6505) was employed to measure the absorbance using glass cells of path length 1 Cm. The morphologies of the catalyst were taken by

**Apparatus**

Fig.1 shows the schematic diagram of photoreactor which was used for photocatalytic decomposition of AR14. In this equipment, capacity 0.5 L with a mercury lamp Philips

SEM model MIRA3 TESCAN and TEM model EM10C–Zeiss. The FT-IR spectroscopy was measured on PerkinElmer Spectrometric Analyzer using KBr pellets.

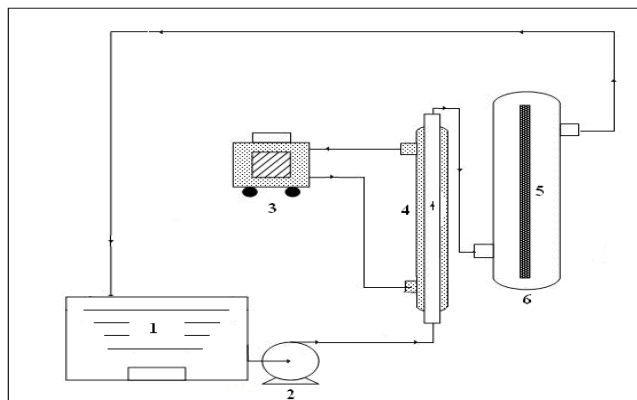


**Figure 1) Schematic diagram of photoreactor**  
1) tank (Pyrex), 2) pump, 3) temperature controller, 4) condenser, 5) UV lamp, 6) reaction flask

### Full factorial experimental design

The photodegradation efficiency of AR14 by MWCNTs particles were investigated using full experimental design. The experiments were designed considering three variables (Factors) including pH, catalyst amount and H<sub>2</sub>O<sub>2</sub> concentration at two levels (low (–) and high (+)). Factorial designs are usually discussed in terms of coded factor spaces. Variables and levels used in 2<sup>3</sup> full factorial experimental design are shown in Table 2. The experiments were carried out by varying the pH 3 to 5, catalyst amount 20 to 30 mg L<sup>-1</sup> and H<sub>2</sub>O<sub>2</sub> concentration 15 to 20 ppm. In this study, classical calculations method was used for the design of experiments and analyzes the results in the process.

**Table 2) Factors and levels used in the 2<sup>3</sup> factorial design.**

Variables (Factors)	Coding	Range and levels	
		Low (–)	High (+)
A) pH	X <sub>1</sub>	3	5
B) Catalyst amount (mg L <sup>-1</sup> )	X <sub>2</sub>	20	30
C) H <sub>2</sub> O <sub>2</sub> concentration (ppm)	X <sub>3</sub>	15	20

### Procedures

For the photodegradation of AR14, a solution containing specific concentration of (40 ppm) and catalyst was prepared. The suspension pH values were adjusted at the desired level using dilute NaOH 0.1N and H<sub>2</sub>SO<sub>4</sub> 0.1N (the pH values were measured with Horiba M12 pH meter) and then were allowed to equilibrate for 30 min in darkness. In order to carry out each experiment (according to Table 3), 0.5 L AR14 solution was made as specified concentration and was transferred to reaction flask (Pyrex). The degradation reaction took place under the radiation of a mercury lamp. The concentration of the samples was determined (at 5 min intervals and centrifuged with centrifuge 4232 ALC) using a spectrophotometer (UV-Vis spectrophotometer, Jenway (6505) at λ<sub>max</sub>=514 nm. The photodegradation efficiency (Y) as a function of time is given by (Eq.1):

$$Y = \frac{(C_0 - C)}{C_0} \times 100, \quad (1)$$

where C<sub>0</sub> and C are the concentration of dye (ppm) at t=0 and t (min), respectively.

### Results

#### The characterization of MWCNTs particles

Fig. 2 shows the SEM image of MWCNTs particles. Regarding to the specified scale in the Fig. 2 size of the particles is nanometer. The size and morphology of MWCNTs powder were characterized.

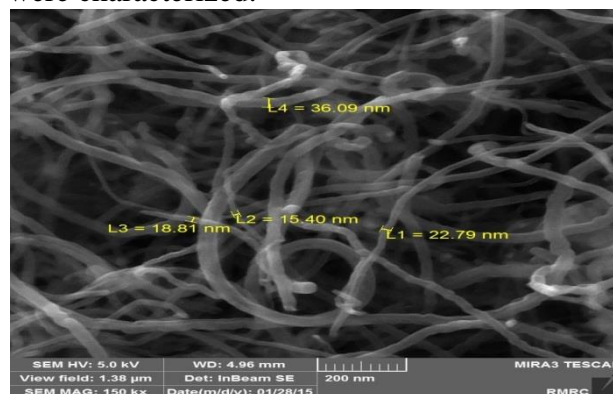


**Figure 2) SEM image of MWCNTs**

Fig. 3 shows the TEM image of MWCNTs powder. The TEM was used due to its ability to measure nanotubes diameter. From the TEM image it is possible to determine directly the diameter of one nanotubes and bundle diameter. Due to this information, a number of nanotubes in the bundle can be found.

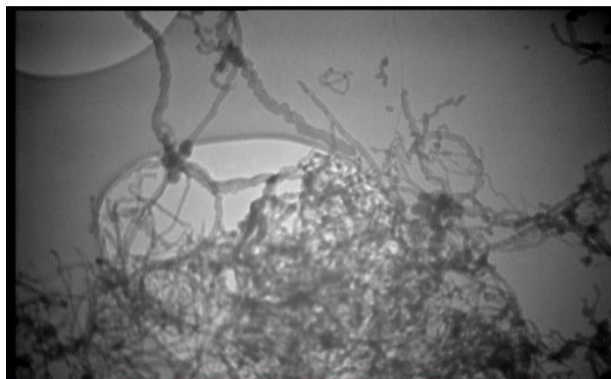


Figure 3) TEM image of MWCNTs

Fig. 4 shows the FT-IR spectrum of MWCNTs particles in the wave number range from 400 to 4000  $\text{cm}^{-1}$ . The bands at 3462 and 1703  $\text{cm}^{-1}$  are due to O-H stretching and O-H bending, respectively. The bands at 2929 and 2873  $\text{cm}^{-1}$  correspond to asymmetric and symmetric aliphatic C-H stretching, respectively. Bands at 1300-1000  $\text{cm}^{-1}$  correspond to C-O and C-C stretching (15).

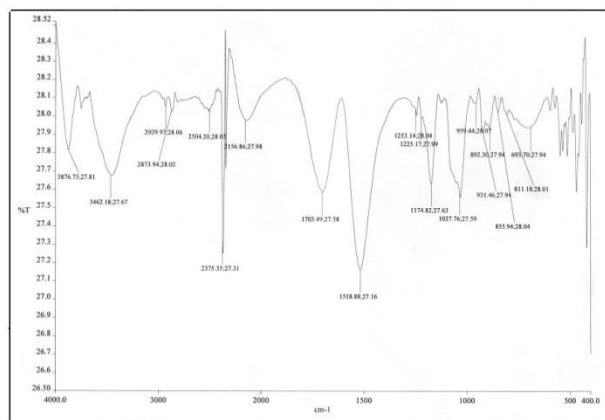


Figure 4) FT-IR spectrum of MWCNTs

### The UV-Vis spectra

The absorbance of AR14 solutions during the process at initial and after 50 min irradiation

time versus wavelength ( $\lambda$ ) are shown in Fig. 5. The spectrum of AR14 in the visible region exhibits a main band with a maximum at 514 nm. The decrease of absorption peaks of AR14 at  $\lambda_{\text{max}}=514$  nm in this figure indicates a rapid degradation of the azo dye. Complete discoloration of dye was observed after 50 min under optimal conditions.

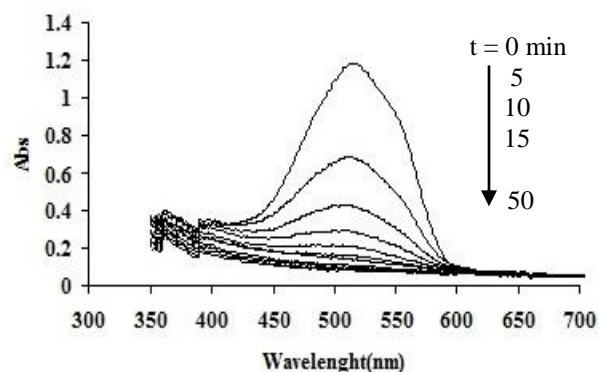


Figure 5) UV-Vis spectra of AR14 on photodegradation (dye concentration= 40 ppm, catalyst amount= 30  $\text{mg L}^{-1}$ ,  $\text{H}_2\text{O}_2$  concentration= 20 ppm, pH= 3,  $T=25^\circ\text{C}$ , irradiation time= 50 min)

### The classical mathematical treatment of a full factorial design

In this study, the experimental design used is a two level and three factors (A, B and C). The design is called a  $2^3$  factorial design, which has 8 experiments. Using the (- and +) notation to represent the low and high levels of the factors; listed the eight experiments in the  $2^3$  design as in Table 3. This is called the design matrix. The first column of Table 3 lists the experiment numbers (1-8). The next three columns list the abbreviated coded factor levels (- and +) for factors A, B and C. Table 4 gives a contrast constants for the  $2^3$  design. The first column of Table 4 gives a notation often used to describe the treatment combinations (TC), where the presence of the appropriate lower-case letter indicates that the factor is at the high level and its absence that the factor is at the low level. The number 1 is used to indicate that all factors are at the low level. The next seven columns list the three factors and four interaction of the

model: the three two-factor interactions (AB, AC and BC), the one three-factor interactions (ABC). Finally, the last column of Table 4 lists

the average responses (photodegradation efficiency (Y)) of the each experiment.

**Table 3) Experimental design matrix, experimental results photodegradation efficiency for AR14 (%).**

Run Number	Factors			Treatment Combination (TC)	Response (Y)
	A	B	C		
1	-	-	-	(1)	66.35
2	+	-	-	a	84.57
3	-	+	-	b	69.42
4	+	+	-	ab	78.19
5	-	-	+	c	83.90
6	+	-	+	ac	73.87
7	-	+	+	bc	90.65
8	+	+	+	abc	81.44

**Table 4) Contrast constants for the (2<sup>3</sup>) design.**

TC	Factors and their interactions							Response (Y)
	A	B	AB	C	AC	BC	ABC	
(1)	-	-	+	-	+	+	-	66.35
a	+	-	-	-	-	+	+	84.57
b	-	+	-	-	+	-	+	69.42
ab	+	+	+	-	-	-	-	78.19
c	-	-	+	+	-	-	+	83.90
ac	+	-	-	+	+	-	-	73.87
bc	-	+	-	+	-	+	-	90.65
abc	+	+	+	+	+	+	+	81.44

In the classical factorial design literature, a factor effect is defined as the difference in average responses between the experiments carried out at the high level of the factor and the experiments carried out at the low level of the factor. Thus, in a 2<sup>3</sup> full factorial design, the main effect of A would be calculated by (Eq.2):  

$$A = (\text{Average responses at high level of A}) - (\text{Average responses at low level of A}) \quad (2)$$

Average responses at high level of A =  

$$1/4 \times (84.57 + 78.19 + 73.87 + 81.44) = 79.5175$$

Average responses at low level of A =  

$$1/4 \times (66.35 + 69.42 + 83.90 + 90.65) = 77.58$$

The main effect of A = 79.5175 - 77.58 = 1.9375.

The interactions effect can be calculated similarly. Therefore, the effect of each factor/interaction is listed in Table 5. The effect of each factor on response was found to be in the following the order: pH (1.9375), catalyst amount (2.7525) and H<sub>2</sub>O<sub>2</sub> concentration

(7.8325). It can be seen that H<sub>2</sub>O<sub>2</sub> concentration has the main effect on response. The least effect factor on the response is pH. The interaction between pH × catalyst amount and pH × catalyst amount × H<sub>2</sub>O<sub>2</sub> concentration have a little effect on response. The interaction between pH × H<sub>2</sub>O<sub>2</sub> concentration and catalyst amount × H<sub>2</sub>O<sub>2</sub> concentration have a great effect on response. Thus the most effect interaction is that between pH × H<sub>2</sub>O<sub>2</sub> concentration (AC).

**Table 5) Effect of each factor/interaction on response.**

Factors/interactions	Effect
A	1.9375
B	2.7525
AB	-2.1575
C	7.8325
AC	-11.5575
BC	4.4075
ABC	2.5675

### The Yates' algorithm

There is a quick way to calculate the effects of factorial design presented by Yates'. The

Yates' algorithm describe here, and illustrate its use for the  $2^3$  full factorial design discussed. To apply the Yates' algorithm, the results should be placed in a standard order. The results are the numerical values of the estimated factor effects. As shown in Table 6, the Yates calculations start by evaluating as many auxiliary columns as factors being considered, in our example three columns E1, E2 and E3 for a  $2^3$  design. The first four elements in column E1 are obtained by adding the pairs together (66.35+84.57=150.92, 69.42+78.19=147.61, etc). The last four elements in column E1 are obtained by

subtracting the top response from the bottom response of each pair, thus 84.57– 66.35=18.22, 78.19 – 69.42= 8.77, and so on. In just the same way that column E1 is obtained from the "Response" column, column E2 is obtained from column E1 and column E3 is obtained from column E2. Finally, obtain the "Effect" column have only to divide these values by the appropriate divisor, as before, which is 8 (the number of runs) for the first element and 4 (half of the runs) for the others. Calculations can be made sure that the first value in column E3 (628.39) is the sum of all the responses.

**Table 6) Yates's algorithm for the  $2^3$  factorial design.**

Run Number	TC	Response	E1	E2	E3	Divisor	Effect
1	None	66.35	150.92	298.53	628.39	8	78.5487
2	a	84.57	147.61	329.86	7.75	4	1.9375
3	b	69.42	157.77	26.99	11.01	4	2.7525
4	ab	78.19	172.09	-19.24	-8.63	4	-2.1575
5	c	83.90	18.22	-3.31	31.33	4	7.8325
6	ac	73.87	8.77	14.32	-46.23	4	-11.5575
7	bc	90.65	-10.03	-9.45	17.63	4	4.4075
8	abc	81.44	-9.21	0.82	10.27	4	2.5675

**The statistical analysis**

The statistically significant variables were tested using analysis of variance (ANOVA). It can be shown that in a two-level experiment, like this one, the sum of squares (SS) for the  $2^3$  full factorial design is given by (Eq.3):

$$SS_{(factor/interaction)} = N/4 \text{ (the estimate effect of factor/interaction)}^2, \tag{3}$$

where N is the total number of measurements, including replicates. In this case N is 16 since two replicate measurements were made for each combination of factor levels. For example  $SS_A$  is:

$$SS_A = 16/4 (1.9375)^2 = 15.0156$$

It can be shown that each sum of squares has one degree of freedom (DOF). Since the mean square (MS) is given by (Eq.4):

$$MS = SS/DOF \tag{4}$$

Each MS is simply the corresponding SS. For example  $MS_A$  is:

$$MS_A = 15.0156/1 = 15.0156$$

To test for the significance of an effect, the MS is compared with the error mean square (EMS) or residual mean square (RMS). RMS values are listed in Table 7.

**Table 7) RMS values for the  $2^3$  factorial design.**

Run Number	TC	(1)	(2)	(3)
1	None	65.35	67.35	132.7
2	a	83.57	85.57	169.14
3	b	68.42	70.42	138.84
4	ab	77.19	79.19	156.38
5	c	82.90	84.90	167.8
6	ac	72.87	74.87	147.74
7	bc	89.65	91.65	181.3
8	abc	80.44	82.44	162.88

In Table 7, columns (1) and (2) are the values of each experiment that are repeated. Column (3) is the sum of the values of columns (1) and (2). RMS value is given by (Eq.5):

$$\text{RMS} = ((65.35)^2 + (83.57)^2 + \dots + (80.44)^2 + (67.35)^2 + (85.57)^2 + \dots + (82.44)^2 - 1/2 (132.7)^2 + (169.14)^2 + \dots + (162.88)^2) = 16. \quad (5)$$

In order to test whether the difference between MS and RMS is significant, the calculated statistic F is given by (Eq.6):

$$F_{\text{calculated}} = \text{MS}/\text{RMS}. \quad (6)$$

The critical value is  $F_{1,8}=5.318$  ( $P=0.05$ ). If  $F_{\text{calculated}} > F_{\text{critical}}$ , then the effect is significant. For example  $F_{(A) \text{ calculated}}$  is:

$$F_{(A) \text{ calculated}} = \text{MS}_A/\text{RMS} = 15.0156/16 = 0.9384.$$

The results of ANOVA are listed in Table 8. Table 8 shows that the main factor such as  $\text{H}_2\text{O}_2$  concentration is significant. Also interaction between  $\text{pH} \times \text{H}_2\text{O}_2$  concentrations is significant. Thus the factor of  $\text{H}_2\text{O}_2$  concentration and interaction between  $\text{pH} \times \text{H}_2\text{O}_2$  concentrations are significant.

Table 8) ANOVA table for the  $2^3$  factorial design.

Factor/interaction	SS	DOF	MS	F	Result
A	15.0156	1	15.0156	0.9384	no sig.
B	30.3050	1	30.3050	1.8940	no sig.
AB	18.6192	1	18.6192	1.1637	no sig.
C	245.3922	1	245.3922	15.3370	significant
AC	534.3032	1	534.3032	33.3939	significant
BC	77.7042	1	77.7042	4.8565	no sig.
ABC	26.3682	1	26.3682	1.6480	no sig.
Error		8			
Total		15			

### The regression model

In a  $2^3$  factorial design, it is easy to express the results of the experiment in terms of a regression model. Because the  $2^3$  is just a factorial design, can be also use either an effects or a means model. A first order regression model is given by (Eq.7):

$$\hat{Y} = b_0 + b_3X_3 + b_{13}X_1X_3, \quad (7)$$

where  $\hat{Y}$  is the predicted photodegradation efficiency,  $b_0$  the average response,  $b_3$  the

regression coefficient and  $b_{13}$  is interaction coefficient. The coded variable  $X_3$  is represent  $\text{H}_2\text{O}_2$  concentration. The  $X_1X_3$  term is the interaction between  $\text{pH} \times \text{H}_2\text{O}_2$  concentration. The coded variable  $X_1, X_3$  take on values between  $-1$  and  $+1$ . The  $\hat{Y}$  at run (1) is:

$$\hat{Y} = 78.5487 + (7.8325/2)(-1) - (11.5575/2)(-1)(-1) = 68.8538.$$

Residuals can be obtained as the difference between experimental and predicted etches rate deviations. The residual is given by (Eq.8):

$$e = Y - \hat{Y}. \quad (8)$$

The values of  $Y, \hat{Y}$  and  $e$  are listed in Table 9. Table 9 shows that  $\text{H}_2\text{O}_2$  concentration and interaction between  $\text{pH} \times \text{H}_2\text{O}_2$  concentrations are the significant effects and that the underlying assumptions of the analysis are satisfied.

Table 9) Values of  $Y, \hat{Y}$  and  $e$  for the  $2^3$  factorial design.

Run Number	TC	$Y$	$\hat{Y}$	$e = Y - \hat{Y}$
1	(1)	66.35	68.8538	-2.5038
2	a	84.57	80.4112	4.1588
3	b	69.42	68.8538	0.5662
4	ab	78.19	80.4112	-2.2212
5	c	83.90	88.2436	-4.3436
6	ac	73.87	76.6862	-2.8162
7	bc	90.65	88.2436	2.4064
8	abc	81.44	76.6862	4.7538

### The kinetic of photocatalytic degradation of dye

Photocatalytic degradation reaction kinetic of dye completely correspond the kinetic of pseudo first order reaction model (16, 17). In the kinetic equation of first order relationship between  $[dye]$  and time ( $t$ ) is in (Eq.9):

$$\text{dye} \xrightarrow{k} \text{product}$$

$$\frac{-d[dye]}{dt} = k[dye], \quad (9)$$

The integral Eq.9 is in Eq.10:

$$\frac{-d[\text{dye}]}{dt} = k[\text{dye}] \rightarrow \frac{d[\text{dye}]}{[\text{dye}]} = -kdt \rightarrow \int_{[\text{dye}]_0}^{[\text{dye}]} \frac{d[\text{dye}]}{[\text{dye}]} = -k \int_0^t dt \Rightarrow \ln[\text{dye}] - \ln[\text{dye}]_0 = -kt \Rightarrow \ln \frac{[\text{dye}]_0}{[\text{dye}]} = kt. \quad (10)$$

In which  $k$  is the apparent first order rate constant (that is affected by  $[\text{dye}]$ ) and  $t$  is the reaction time.

A plot of  $\ln\left(\frac{[\text{dye}]_0}{[\text{dye}]}\right)$  versus  $t$  for optimum condition of photocatalytic degradation of dye is shown in Fig. 6. The linear plot suggests that the photodegradation reaction approximately follows the pseudo first order kinetic with a rate constant  $k = 0.0696 \text{ min}^{-1}$ .

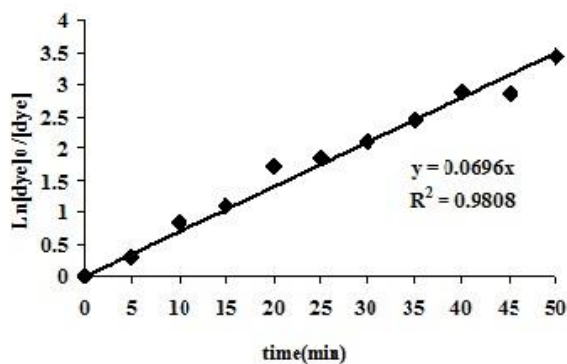


**Figure 6) Kinetics of photocatalytic degradation of AR14 (dye concentration= 40 ppm, catalyst amount= 30 mg L<sup>-1</sup>, H<sub>2</sub>O<sub>2</sub> concentration= 20 ppm, pH= 3, T= 25 °C, irradiation time= 50 min)**

The half-life time ( $t_{1/2}$ ) for the first order reaction is given by (Eq.11):

$$t_{1/2} = \frac{0.693}{k} \quad (11)$$

So, a first order reaction with half-life time ( $t_{1/2} = 9.956 \text{ min}^{-1}$ ) was observed for the photocatalytic degradation reaction.

## Discussion

In this study, for degradation of dye as dangerous pollutants used a photoreactor with capacity 0.5 L that shows the schematic diagram in Fig.1. The photodegradation process using full factorial experimental design was studied by many investigators (18-20). The maximum photodegradation efficiency of AR14 obtained in this study was found to be 90.65%, corresponding to the operating conditions of 3, 30 mg L<sup>-1</sup> and 20 ppm respectively, for the pH, catalyst amount and H<sub>2</sub>O<sub>2</sub> concentration. The positive signs (run number: 7, Table 3) are related to factors such as: catalyst amount and H<sub>2</sub>O<sub>2</sub> concentration. The increase in catalyst amount increases the surface area available by more photocatalyst particles. So, the number of active sites on the photocatalyst surface increases that leads to the increase of the photocatalytic degradation efficiency (21). The effect of H<sub>2</sub>O<sub>2</sub> concentration on the photodegradation efficiency of dye was performed at a range 15 ppm or 20 ppm. The photodegradation efficiency increases with increase of H<sub>2</sub>O<sub>2</sub> concentration. This can be explained by the effect of the additionally produced hydroxyl radicals (22,23).

The negative sign (run number: 7, Table 3) is related to factor pH. The photodegradation efficiency of AR14 at pH with levels 3 and 5, which the best results obtained in acidic solution, (pH= 3, X= 90.65%). The charge of catalyst and its surface is presumably positively charged in acidic solution and negatively charged in alkaline solution. For the above reasons, dye that has a sulfonic groups (SO<sub>3</sub><sup>-</sup>) in its structure, which is negatively charged, the acidic solution favors adsorption of dye onto the photocatalyst surface, thus the photodegradation efficiency increases. This effect is in agreement with the results of Sato, Yoneyama and Nikazar (24-26). In a experiments result indicated that the degradation rate of dye in this process fitted by the first order kinetic model (16,17).



## Conclusion

Azo dyes have been widely used in different industries. Wastewater industries cause environmental pollutant problems. So, industries wastewater treatment plan are necessary. MWCNTs particles have been characterized by SEM, TEM and FT-IR. The full factorial experimental design based design matrix and Yates' algorithm were used in this process. As observed, the most effective factors in the photocatalytic degradation efficiency were  $H_2O_2$  concentration. pH was the least effect factor on the response. The interaction between pH $\times H_2O_2$  concentration was the most influencing interaction. The results of ANOVA shows that the main factor such as:  $H_2O_2$  concentration is significant. Also interaction between pH $\times H_2O_2$  concentration are significant. Thus the factor of  $H_2O_2$  concentration and interaction between pH $\times H_2O_2$  concentration are highly significant. The regression model was studied. Kinetics of photocatalytic decomposition reaction was determined. Pseudo first order model reaction corresponds to the experiment data of photocatalytic degradation of dye was observed.

## Footnotes

### Acknowledgement:

The authors wish to acknowledge members of the Research Laboratory of Islamic Azad University, Arak Branch, Arak, Iran.

### Conflict of Interest:

The Authors have no conflict of interest.

## References

1. Venkataraman K. The chemistry of synthetic dyes. New York: Academic Press; 1970. p. 169. (vol 3)
2. Zollinger H. Color Chemistry Synthesis, Properties, and Applications of Organic Dyes and Pigments. 3rd Ed. New York: Wiley; 2003. p. 298.
3. Bayramoglu G, Arica MY. Enzymatic removal of phenol and p-chlorophenol in enzyme reactor:

horseradish peroxidase immobilized on magnetic beads. J Hazard Mater 2008;156(1-3):148-155.

4. Tepe O, Dursun AY. Combined effects of external mass transfer and biodegradation rates on removal of phenol by immobilized *Ralstonia eutropha* in a packed bed reactor. J Hazard Mater 2008;151(1):9-16.

5. Kaviani D, Asadi M, Khodabakshi MJ, Rezaei Z. Removal of Malachite Green dye from aqueous solution using  $MnFe_2O_4/Al_2O_3$  nanophotocatalyst by UV/ $H_2O_2$  process. Arch Hyg Sci 2016;5(2):75-84.

6. Shokri A. Application of Sonocatalyst and Sonophotocatalyst for Degradation of Acid Red 14 in Aqueous Environment. Arch Hyg Sci 2016;5(4):229-235.

7. Nazari Sh, Yari AR, Mahmoodian MH, Tanhaye Reshvanloo M, Alizadeh Matboo S, Majidi Gh, et al. Application of  $H_2O_2$  and  $H_2O_2/FeO$  in removal of Acid Red 18 dye from aqueous solutions. Arch Hyg Sci 2013;2(3):114-120.

8. Yari AR, Alizadeh M, Hashemi S, Biglari H. Efficiency of electrocoagulation for removal of Reactive Yellow 14 from aqueous environments. Arch Hyg Sci 2013;2(1):7-15.

9. Bach A, Semiat R. The role of activated carbon as a catalyst in GAC/iron oxide/ $H_2O_2$  oxidation process. Desalination 2011;273(1):57-63.

10. Yeddou AR, Nadjemi B, Halet F, Ould-Dris A, Capart R. Removal of cyanide in aqueous solution by oxidation with hydrogen peroxide in presence of activated carbon prepared from olive stones. Minerals Eng 2010;23(1):32-39.

11. Santos VP, Pereira MFR, Faria PCC, Orfao JJ. Decolourisation of dye solutions by oxidation with  $H_2O_2$  in the presence of modified activated carbons. J Hazard Mater 2009;162(2-3):736-742.

12. Ren XM, Chen CL, Nagatsu M, Wang XK. Carbon nanotubes as adsorbents in environmental pollution management: A review. Chem Eng J 2011;170(2-3):395-410.

13. Torkaman M, Moradi R, Keyvani B. Photocatalytic degradation azo dye Direct Red 23 using carbon nanotubes particles by UV/ $H_2O_2$  Process in batch photoreactor. Rev Roum Chim 2016;61(10):763-772.

14. Miller JN, Miller JC. Statistics and Chemometrics for Analytical Chemistry. 5th Ed. London: Prentice Hall; 1944.

15. Hejun G, Siyuan Z, Xiyuan C, Xiaodong W, Liqiang Z. Removal of anionic azo dyes from aqueous solution using magnetic polymer multi-wall carbon nanotube nanocomposite as adsorbent. Chem Eng J 2013;223(1):84-90.

16. Muruganandham M, Swaminathan M. Photochemical oxidation of reactive azo dye with UV- $H_2O_2$  process. Dyes Pigments 2004;62(3):269-275.

17. Amin MM, Golbini Mofrad MM, Pourzamani H, Sebaradar SM, Ebrahim K. Treatment of industrial

wastewater contaminated with recalcitrant metal working fluids by the photo-Fenton process as post-treatment for DAF. *J Indus Eng Chem* 2017;45(1):412-420.

18. Saghi M, Mahanpoor K. Photocatalytic degradation of tetracycline aqueous solutions by nanospherical  $\alpha$ -Fe<sub>2</sub>O<sub>3</sub> supported on 12-tungstosilicic acid as catalyst: using full factorial experimental design. *Int J Ind Chem* 2017;8(3):297-313.

19. Alizadeh Kordkandi S, Forouzes M. Application of full factorial design for methylene blue dye removal using heat-activated persulfate oxidation. *J Taiwan Ins Chem Eng* 2014;45(5):2597-2605.

20. Barka N, Abdennouri M, Boussaoud A, Galadi A, Baalala M, Bensitel M, Sahibed-Dine A, Nohair K, Sadiq M. Full factorial experimental design applied to oxalic acid photocatalytic degradation in TiO<sub>2</sub> aqueous suspension. *Arabian J Chem* 2014;7(5):752-757.

21. Seyyedi K, Farbodnia Jahromi MA. Decolorization of azo dye C.I. Direct Black 38 by Photocatalytic method using TiO<sub>2</sub> and optimizing of process. *APCBEE Procedia* 2014;10:115-119.

22. So CM, Cheng MY, Yu JC, Wong PK. Degradation of azo dye Procion Red MX-5B by photocatalytic oxidation. *Chemosphere* 2002;46(6):905-912.

23. Lee JM, Kim MS, Hwang B, Bae W, Kim BW. Photodegradation of acid red 114 dissolved using a photo-Fenton process with TiO<sub>2</sub>. *Dyes Pigments* 2003;56(1):59-67.

24. Sato S. Effects of surface modification with silicon oxides on the photochemical properties of powdered titania. *Langmuir* 1988;4(5):1156-1159.

25. Yoneyama H, Haga Sh, Yamanaka Sh. Photocatalytic activities of microcrystalline titania incorporated in sheet silicates of clay. *J Phys Chem* 1989;93(12):4833-4837.

26. Nikazar M, Gholivand Kh, Mahanpoor K. Photocatalytic degradation of azo dye Acid Red 114 in water with TiO<sub>2</sub> supported on clinoptilolite as a catalyst. *Desalination* 2008;219(1-3):293-300.